

# Frequency locking and travelling bursts sequences in modular network of inhibitory neurons with differing time-scales

Kunal Mozumdar<sup>1</sup> and G. Ambika<sup>1</sup>

Indian Institute of Science Education and Research, Pune, India - 411008

Received: date / Revised version: date

**Abstract.** We report the emergent dynamics of a community structured modular network of chaotic Hindmarsh-Rose neurons with inhibitory synapses. We find the inhibitory coupling between the neuronal modules leads to complete synchronization of neurons in a module, and also pushes modules into interesting sequence of *travelling burst patterns*. When differing dynamical time-scales are introduced for neurons in each module, hence breaking the symmetry between them, we see specific sequences of travelling burst patterns that are characteristic of the time-scale mismatch and coupling strengths. For a modular network with only two time-scales, the neuronal sub-ensembles enter into *synchronized frequency locked clusters* with the bursting sequences having recurring patterns. Our results have significance in the process of information coding in terms of frequency of firing dynamics among neurons and in selective communication based on the sequences of bursts.

**PACS.** 87.19.lj Neuronal Network Dynamics – 05.45.Xt Synchronization, Coupled Oscillators – 82.39.Rt Complex Biological Systems – 87.19.lp Pattern Formation in Neuroscience

## 1 Introduction

Studies related to the brain and its various structural and dynamical features have been a very interesting and challenging area of research in recent times. This is mainly because the brain is highly complex with over  $10^9$  neurons connected via complex networks perfected by evolution. Although reproducing the dynamics of the brain is close to impossible due to its intricate connectome and constituent levels of its complexity, there are several generalizations in the neuronal architecture and dynamical features in the brain. These generalizations can be abstracted to give very useful mathematical models of neuronal networks, which can be extended to model the real structures in the brain. [1, 2, 3, 4]. Neuronal networks dynamically self-organize in various length and time-scales to give rise to a wide repertoire of behaviours. While the dynamical state of an individual neuron depends on the type of ion channels, their dendritic structure and the nature of coupling with other neurons, the complex behavioural aspects produced by the brain are due to the collective dynamics of several ensembles of neurons [5, 6].

In this context, modular networks are one of the quite commonly found network topology in the brain. Modular networks consist of nodes that are classified into certain groups or communities based on some characteristics of the nodes or based on their connections with other nodes

[7, 8]. There has been a lot of connectomics study which have pointed to the modular organization of the networks in the mammalian brain [9, 10, 11]. Some notable examples of modular architecture are the striatal networks, visual cortex and olfactory lobes in mammals [12] and also the layers of neurons in medial entorhinal cortex [13, 14]. Various studies have shown that this type of structure may have some role in processing of information in neural circuits [15]. Some theoretical studies also explore the potential aspects of the modular organization leading to interesting dynamical phenomena in neuronal networks [16, 17, 18].

The dynamical features of individual neurons like spiking and bursts are captured by several nonlinear dynamical models, the most widely used among them being Hindmarsh - Rose neuronal model [19] that can demonstrate a wide class of bursting dynamics [20, 21]. As is well established neurons can make contacts with other neurons through synapses that can be excitatory or inhibitory. Specifically, several studies report the effect of inhibitory synaptic connections in neurons [22, 23, 24, 25, 26] and this type of coupling is found very crucial in producing rhythmic activity in the brain [27, 28, 29, 30].

Along with the nature of connectivity among the neurons, the major factor affecting the neuronal dynamics is the *time-scale of neuronal activity*. The time-scale of neuronal dynamics is generally dependent on the interplay of

the various ions flowing across the cell membrane of the neuron deciding its capacitance and conductance [31]. The collective activities of neurons are heavily dependent on the temporal scales of activity of each individual neuron or ensembles of neurons [32, 13, 33, 34, 35] and they tend to play a major role in the oscillations in the mid brain region [27].

We address an important aspect of brain dynamics, viz how the presence of differing time-scales affect the emergent dynamics of the modular neuronal networks. This is carried out by incorporating the multiple time-scales in the dynamics of the neurons as a time-scale parameter in the dynamics of HR neurons [36]. We start with the hypothesis that the presence of differing time-scales and inhibitory coupling can result in modulation of emergent frequencies in the system. We present a comprehensive model of a system where such variations in burst frequencies and emergence of frequency locked clusters can be studied in detail for a range of parameter values. We note that such modulation of oscillation frequencies and frequency locking have been observed from MEG/EEG data [37] and intra-cortical recordings [38] in primates and rats. Furthermore they may have a vital role in the formation of working memory.

The modular network that we present is a very basic model that can address the dynamical complexity of the brain. It illustrates how a system of Hindmarsh-Rose neurons can produce travelling burst sequences that circulate periodically among the modules. We observe a variety of dynamical states when the time-scales of the dynamics in the modules are varied. The most relevant among them are the frequency-synchronized clusters with periodic sequences of bursting evident from the spatio temporal dynamics of the network.

The model and methods of study are introduced in the next section. The results of our analysis on modular networks with identical neurons and those with time scale mismatch in their dynamics are detailed in the next three sections. The salient features and main results of the study are summarized in the final section.

## 2 Modular Neuronal Networks with differing time-scales

We start with a model of community structured network consisting of  $N$  neurons grouped into  $M$  modules or communities. This is set up by choosing the elements  $a_{ij}$  of the  $N \times N$  connectivity matrix as :

$$a_{ij} = \begin{cases} b_{ij}, \forall i \bmod (N/M) = j \bmod (N/M) \\ b'_{ij}, \forall i \bmod (N/M) \neq j \bmod (N/M) \end{cases} \quad (1)$$

The intrinsic dynamics of each neuron is taken as the Hindmarsh Rose(HR) model and then the dynamics of the

$i^{th}$  neuron in the network evolves as:

$$\begin{aligned} \dot{x}_i = & \eta_i \left( y_i - x_i^3 + 3x_i^2 - z_i + I_e \right. \\ & + g_{in}(V - x_i) \sum_{j=1}^N b_{ij} \left( \frac{1}{e^{-\lambda(x_j + K)}} \right) \\ & \left. + g_{out}(V - x_i) \sum_{j=1}^N b'_{ij} \left( \frac{1}{e^{-\lambda(x_j + K)}} \right) \right), \end{aligned} \quad (2a)$$

$$\dot{y}_i = \eta_i(1 - 5x_i^2 - y_i), \quad (2b)$$

$$\dot{z}_i = \eta_i(\epsilon(4(x_i + x_r) - z_i)) \quad (2c)$$

Here, the variable  $x_i$  represents the membrane potential and the variable  $y_i$  and  $z_i$  represent the fast and slow gating variables of the HR neuron. We use the parameters  $I_e = 3$  and  $\epsilon = 0.006$  such that the intrinsic dynamics shows chaotic bursts. The synaptic coupling function is a sigmoidal function with parameters  $\lambda = 10$ , reversal potential  $V = 2$  and synaptic threshold  $K = 0.25$  respectively. The elements of the connectivity matrix are such that  $b_{ij} = b'_{ij} = 1$  if there is a synaptic connection between neurons  $j$  and  $i$  and zero otherwise. The coupling strengths between neurons inside the modules are represented by  $g_{in}$  and that between inter module synapses by  $g_{out}$ .

The model as such is quite general but in the present study we concentrate on the special case of a modular network with all-to-all inhibitory connections between neurons from any two different communities and no connections among neurons inside each community. Therefore we fix  $g_{out} = -\beta$  with the values of  $b_{ij} = 0$  and  $b'_{ij} = 1$ . The schematic diagram in Figure 1a shows the structure thus chosen. The typical values of the size of the network used in the study are  $N = 120$  and  $M = 4$ .

We introduce additionally a time scale parameter determining the dynamics of each neuron as  $\eta_i$ , with values in the range  $0 < \eta_i \leq 1$ . It is clear that  $\eta_i = 1$  corresponds to the regular neuronal time-scales while any values of  $\eta_i < 1$  would mean the corresponding neuron being slower in dynamics than others while keeping the nature of its intrinsic dynamics the same [36]. Biologically the parameter  $\eta$  can be attributed to the differences in the capacitance of the axonal membranes. Figure 1b shows the dynamics of two HR neurons, one of which has a slower time-scale with  $\eta = 0.5$ .

In this study we keep the time scale of all the neurons in each module at a specific value of the time-scale  $\eta_i$ . So for the whole network, time-scale parameters form a set of  $M$  values,  $\boldsymbol{\eta} = (\eta_1, \eta_2, \eta_3, \eta_4)$ . We initially consider a network that is symmetric both in structure and dynamics with identical neurons with all modules having the same time scale i.e.  $\boldsymbol{\eta}_0 = (1 \ 1 \ 1 \ 1)$ . In this case we analyze the emergent burst patterns of the whole network using spatio-temporal plots. Then we proceed to the more

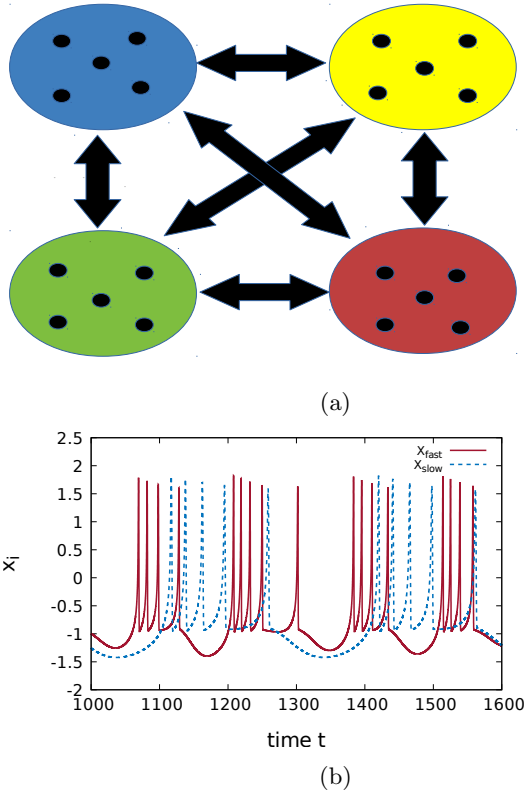


Fig. 1: (Colour Online) **(a) Schematic representation of a network with modular structure:** The circles represent the modules and the dots inside each circle represent the individual neurons. The arrows represent the all-to-all coupling between each neuron in a module with all other neurons in every other module. **(b) Intrinsic dynamics of HR neuron:** The chaotic bursts for parameters  $I_e = 3$  and  $\epsilon = 0.006$  for a neuron (smooth line) with  $(\eta = 1)$  and that for a slow neuron (dotted line) with time-scale mismatch  $\eta = 0.5$

interesting case where one level of symmetry is broken by having two modules follow a slower time scale with a mismatch with the faster ones given by  $\boldsymbol{\eta}_1 = (1 \ \eta \ 1 \ \eta)$  (where  $\eta \in [0, 1)$ ). We also study two other possible configurations with  $\boldsymbol{\eta}_2 = (\eta \ \eta \ \eta \ 1)$  and  $\boldsymbol{\eta}_3 = (1 \ 1 \ 1 \ \eta)$ .

In all cases, the system of equations in (2) is analyzed by numerical simulations using 4<sup>th</sup> order vector Runge-Kutta for a step  $\Delta t = 0.01$  and 600000 iterations. The first 100000 values are discarded as transients and the remaining are used in the analysis. We get the spatio-temporal plots that provide a qualitative picture of the emergent dynamics of the network.

The dynamical activities of neurons can be further characterized quantitatively using the frequencies of bursts. For a detailed characterization of the dynamics, we compute the burst frequency of each neuron from its time series,  $x_i$ . We note the time  $\tau_i^k$  at which the  $x_i$  values cross a threshold value of  $-1.25$  with the  $\dot{x} > 0$ . Thus the

$\tau_i^k$  represents the time of onset of the  $k^{th}$  burst in the  $i^{th}$  neuron. The inter-burst interval (IBI) is then calculated for each burst as the time interval  $\Delta\tau^k = \tau^{k+1} - \tau^k$ . All such  $\tau_i^k$  values are used to calculate the average burst frequency of the  $i^{th}$  neuron using the equation:

$$\omega_i = \frac{2\pi}{K_i} \sum_{k=1}^{K_i} \frac{1}{\tau_i^{k+1} - \tau_i^k} \quad (3)$$

where  $K_i$  refers to the total number of bursts for the  $i^{th}$  neuron in the total time used for calculation. The intrinsic burst frequency of a single HR neuron calculated using this method turns out to be  $f_o \simeq 0.04$  in arbitrary units. This generally corresponds to a frequency of  $\sim 60$  Hz when we compare it with the biological neuronal time series [19].

### 3 Travelling Burst Dynamics

The inhibitory nature of the coupling can produce a tendency for anti-phase synchronization among two neurons because, when one of the neuron is active it tends to inhibit the other neuron's activity. This tendency in a modular network of mutually coupled inhibitory neurons can drive the neurons to enter into a state of sequential bursting. All neurons in a particular community or module are in complete synchrony with each other. So each module of neurons burst one after the other in the same sequence like *travelling bursts*. The spatio-temporal plots in figure 2 illustrate these emergent bursting patterns in the network for two different coupling strengths  $\beta$ .

We can infer a few general trends in the dynamics of the network from the spatio-temporal plots in figure 2. Firstly, the bursting sequence remains periodic as the whole system evolves in time. So inhibitory coupling drives the system of chaotic bursting neurons into a periodic square bursting dynamics. Since the whole network in this case is symmetric, the bursts form a travelling pattern among the modules. Secondly, the bursting dynamics is identical in all modules i.e. all the neurons show a mixed-mode square bursting dynamics, although the bursts are shifted in space and time. Figure 3 shows the time series of typical neurons from each module corresponding to the states of spatio-temporal plots in figure 2.

We calculate the burst frequency of each neuron averaged over the modules. The average burst frequency is the same for a given  $\beta$  indicating frequency synchronization. Moreover, as is clear from the figure 3 also, the time period of each burst increases as  $\beta$  increases. Thus for the case of the symmetric network with identical neurons, with  $\boldsymbol{\eta}_0 = (1 \ 1 \ 1 \ 1)$ , all the neurons are frequency synchronized and the firing pattern has a wave of travelling bursts circulating over the whole network.

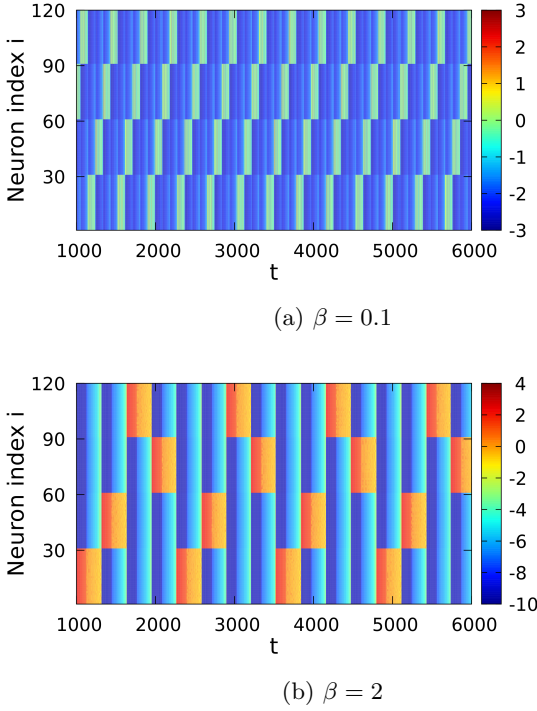


Fig. 2: (Colour Online) **Spatio-temporal plots of the neuronal dynamics:**(a)  $\beta = 0.1$  , (b)  $\beta = 2$ . Each module of neurons bursts sequentially one after the other in time, producing a travelling burst pattern in the network.

#### 4 Bursts sequences with differing time-scales

In this section we present the study on the modular network with a time-scale mismatch between the dynamics of neurons in different modules. The differing time-scales break the symmetry of the network, as now the neurons in one module are non-identical with that in another. We consider the whole network of neurons as divided into equal number of slow and fast systems which are again distributed equally into  $M = 4$  communities. There are thus two slow communities and two fast ones with the time-scales fixed as  $\eta_1 = (1 \ \eta \ 1 \ \eta)$ .

Our numerical analysis shows that in this case also, the travelling burst pattern occurs with the neurons in each module bursting sequentially one after the other. But the pattern of bursting is highly specific to the value of the time-scale  $\eta$ . Moreover now the bursting sequence of each community of neurons in this case now is dependent on which communities are slow and which are fast. This is evident from the spatio-temporal dynamics on the network as shown in figure 4, for three different values of  $\eta$ . For  $\eta = 0.9$ , we identify the sequence of the travelling bursts from figure 4a as  $P_1^{\eta_1} = \overline{S_1 S_2 F_1 F_2}$ , numbered according to the order in which communities burst in time. The bar over the sequence indicates that the sequence is repeated periodically in time.

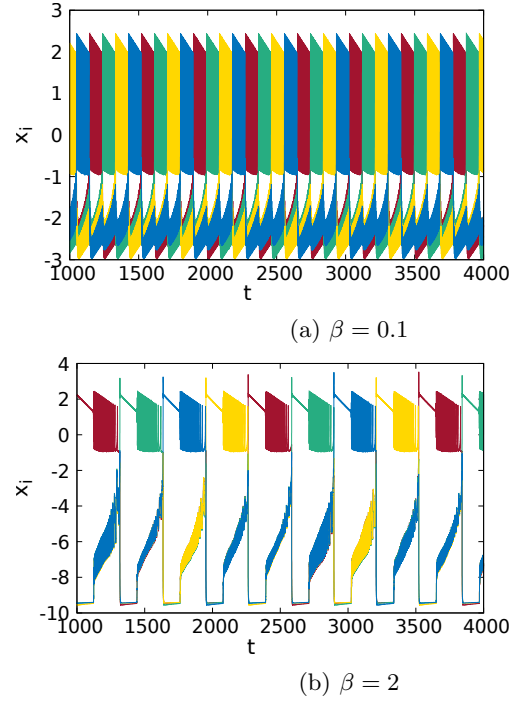


Fig. 3: (Colour Online) **Time series of sequentially bursting neurons from each module:**(a)  $\beta = 0.1$  , (c)  $\beta = 2$ . The dynamics of typical neurons from each community ( for  $i = 30, 60, 90, 120$ ) is shown. It is clear that all neurons have the same periodic bursts that form a sequential pattern of bursting. With the increase in  $\beta$ , the time period of the burst increases.

But at lower values of  $\eta$  like in 4c, ( $\eta = 0.4$ ) the bursting pattern changes to  $P_3^{\eta_1} = \overline{S_2 F_2 F_1 S_1 F_2 F_1}$  so that the slower modules burst once each and the faster modules burst twice in one cycle. For an intermediate value of  $\eta = 0.8$ , the travelling bursts have a longer sequence  $P_2^{\eta_1} = \overline{F_1 S_1 F_2 S_2 F_1 F_2 S_1 F_1 S_2 F_2}$  with slow communities bursting 4 times and fast communities bursting 6 times during the time of one cycle. In all cases, the sequences are repeated periodically in time. At this stage we identify the periodic bursting sequences using the number of slow bursts  $p$  to that of fast bursts  $q$  in a period as  $(p : q)$ . Thus with time scales fixed as  $\eta_1 = (1 \ \eta \ 1 \ \eta)$ , the network has 3 different emergent dynamical states, with burst sequences denoted by  $(2 : 4)$ ,  $(4 : 6)$  and  $(2 : 2)$  for increasing values of  $\eta$ .

We now turn to two more possible configurations of the network that are more heterogeneous with unequal number of slow and fast modules. These give rise to more interesting patterns of burst sequences. For the two possible configurations distinct from those given above, the emergent dynamical sequences and the range of  $\eta$  values for which they are stable are mentioned below. Thus with 3 slow and 1 fast modules ( $\eta_2 = (\eta \ \eta \ \eta \ 1)$ ), the bursting sequences observed are :

$$- P_1^{\eta_2} = \overline{F S_3 F S_2 F S_1} \text{ for } \eta \in [0.3, 0.53] \ (3 : 3)$$

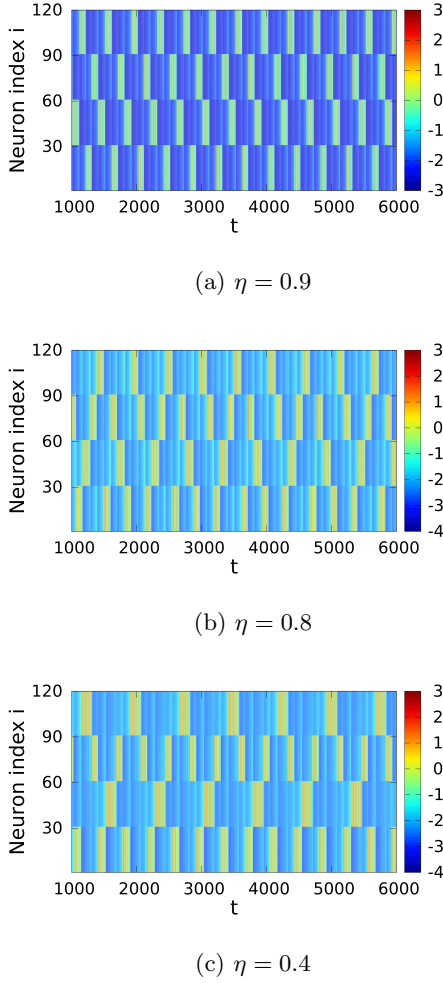


Fig. 4: (Colour Online) **Spatio-temporal plots of the neuronal dynamics with time-scale mismatch at  $\beta = 0.1$ :** (a)  $\eta = 0.9$ , shows the sequence  $P_1^{\eta_1}$ . (b)  $\eta = 0.8$ , shows the sequence  $P_2^{\eta_1}$ . (c)  $\eta = 0.4$  shows the sequence  $P_3^{\eta_1}$ .

- $P_2^{\eta_2} = \overline{S_3 F S_2 S_1 F}$  for  $\eta \in [0.54, 0.59]$  (3 : 2)
- $P_3^{\eta_2} = \overline{F S_3 S_2 F S_1 S_3 F S_2 S_1 F}$  for  $\eta \in [0.6, 0.83]$  (6 : 4)
- $P_4^{\eta_2} = \overline{S_3 S_2 S_1 F}$  for  $\eta \in [0.83, 1]$  (3 : 1)

For the configuration of the network case with 1 slow and 3 fast modules ( $\eta_3 = (1 \ 1 \ 1 \ \eta)$ ), the sequences observed are :

- $P_1^{\eta_3} = \overline{F_3 F_2 F_1}$  for  $\eta \in [0.3, 0.64]$  (0 : 3) (the inhibitory coupling prevents the slow modules from bursting)
- $P_2^{\eta_3} = \overline{S F_3 F_2 F_1 F_3 F_2 F_1 F_3 F_2 F_1}$  for  $\eta \in [0.64, 0.66]$  (1 : 9)
- $P_3^{\eta_3} = \overline{S F_1 F_3 F_2 F_1 F_3 S F_2 F_1 F_3 F_3 F_1 S F_3 F_2 F_1 F_3 F_2}$  for  $\eta \in (0.66, 0.72)$  (3 : 15)
- $P_4^{\eta_3} = \overline{S F_3 F_1 F_2 F_3 S F_1 F_2 F_3 F_1 S F_2 F_3 F_1 F_2}$  for  $\eta \in (0.72, 0.78)$  (3 : 12)
- $P_5^{\eta_3} = \overline{F_3 F_2 F_1 S}$  for  $\eta \in (0.78, 1]$  (1 : 3)

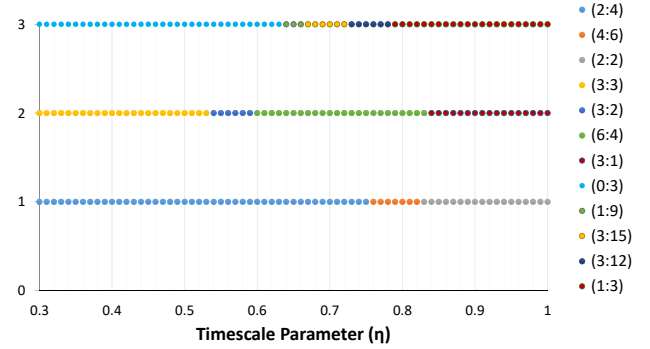


Fig. 5: (Colour Online) **Range of  $\eta$  values for the burst sequences observed in the three configurations of the modules for  $\beta = 0.1$  :** Here line 1 corresponds to the case  $\eta_1$ , 2 corresponds to  $\eta_2$  and 3 corresponds to  $\eta_3$ . For each case the dots of each colour represent a particular sequence of bursts (mentioned on the right) and the respective range of  $\eta$  values.

In a network of 4 modules, these exhaust all possible configurations. We have summarized these results in figure 5 highlighting the ranges of  $\eta$  values for each burst sequence for all the three cases in 4 modules. By extending the study along similar lines to networks with larger number of modules, it is possible to enumerate a variety of interesting periodic patterns of bursting based on the numbers of slow and fast modules and the distribution of  $\eta$  values among them.

## 5 Frequency Locked Clusters

The pattern of sequences reported in section 4 can be further quantified by calculating the average burst frequency for each community of neurons as  $\mathbf{f} = (f_1 \ f_2 \ f_3 \ f_4)$  using equation (3). For the case of two slow and two fast modules, the frequencies for different  $\eta$  values with  $\beta = 0.1$  for each module is shown in 6a. It is clear that for sufficiently small mismatch or large  $\eta$ , all the modules in the network are still in a single frequency synchronized state with the average frequency much less than the intrinsic value. This frequency suppression increases with increasing coupling strength  $\beta$ . As  $\eta$  is reduced, we find the single frequency state bifurcates into a state where the two slow and the two fast modules separate into two different clusters of differing frequencies, while being synchronized among them.

We find that the bursts in the slow and fast modules are locked into specific ratios. This ratio  $\rho$ , of the average frequency of neurons in the slow modules and that

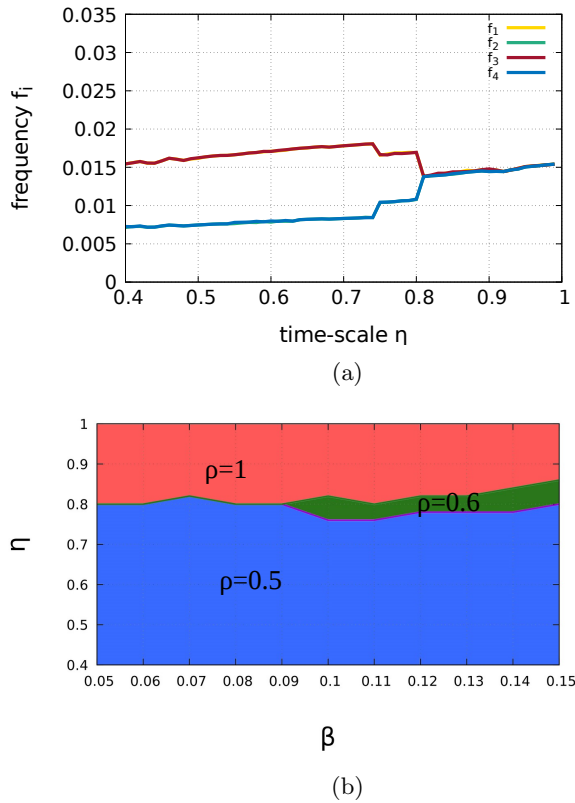


Fig. 6: (Colour Online) **(a) Frequency vs  $\eta$  at  $\beta = 0.1$  for configuration  $\eta_1$ :** The frequencies are suppressed compared to the intrinsic frequency  $f_o$ . Also there are distinct clusters of slow and fast frequencies at lower values of  $\eta$ . **(b) Regions in the  $(\beta, \eta)$  parameter space for configuration  $\eta_1$ :** The three regions correspond to the three distinct *synchronized frequency locked states* - Red(Gray) region corresponds to the State  $\rho = 1$ , Green(Black) region to  $\rho = 0.6$  and Blue(Dark Gray) region to  $\rho = 0.5$ .

of neurons in the fast modules, can thus characterize the locked states. For the network with two slow and two fast modules, we get three distinct ratios, 1, 0.5 and 0.6. The values of the parameters for which the locked states stabilize, are indicated in the parameter plane  $(\beta, \eta)$  in figure 6b.

These frequency locked states correspond directly to the three patterns of burst sequences mentioned above and seen in the spatio-temporal plots in figure 4. Thus  $\rho = 1$  corresponds to the state (2 : 2),  $\rho = 0.5$  corresponds to state (2 : 4) and  $\rho = 0.6$  corresponds to the state (4 : 6). Also we note that while the frequency values of each cluster keep changing with  $\beta$  and  $\eta$ , the locking ratio remains constant over a sufficient region of the plane.

## 6 Discussions

In this study we report the emergent dynamics and bursting patterns produced in a modular network of identical neurons with inhibitory couplings. The burst patterns can be useful for the rhythmic and functional activities of the brain and modular networks are organized from the point of view of pattern formation in the collective dynamics. Our study emphasizes the role of inhibitory couplings in producing regulated patterns of synchrony among neurons.

We show that a variety of dynamical states are possible when the time-scales of the dynamics in the communities are different. Moreover the travelling burst dynamics observed in this case is specific to the mismatch in time scales and can be uniquely characterized by the frequency ratios. The slow and fast time-scales in each module result in specific emergent frequencies in it, which in the presence of inhibitory couplings among them, drive the whole network to fire at various patterns of bursting sequences. By changing the time-scale mismatch parameter, we observe frequency-synchronized clusters that are locked into ratios like 1, 0.5 and 0.6 etc. and are stable over a finite region of the parameter plane of time-scale and coupling strength.

As is well known, the frequency of bursting or firing in the dynamics of connected neurons has a major role in the coding and transmission of information among them [39, 40, 41] especially in selective communication [42]. Also frequency locking and modulation are associated with integrating sensory information to form working memory and retrieval of such memory for sensory guided tasks [43, 44]. In response to input currents, synaptic strengths and heterogeneous synapses, modulation in frequency and frequency-locked states have been reported earlier [45, 46, 47]. But frequency locking and bursting sequences combining temporal and spatial dynamics due to heterogeneous time-scales is a novel phenomenon reported in this work.

By extending the model to larger number of modules and varying the time scale mismatches among them, a variety of sequences can be generated. These bursting sequences themselves can thus be a mechanism or medium for coding information.

## References

1. E. Bullmore, O. Sporns, Nature Reviews Neuroscience **10**(3) (2009)
2. E.M. Izhikevich, *Dynamical systems in neuroscience* (MIT press, 2007)
3. P. Ashwin, S. Coombes, R. Nicks, The Journal of Mathematical Neuroscience **6**(1), 2 (2016)
4. D. Parker, V. Srivastava, Frontiers in physiology **4** (2013)
5. T. Womelsdorf, J.M. Schoffelen, R. Oostenveld, W. Singer, R. Desimone, A.K. Engel, P. Fries, science **316**(5831), 1609 (2007)

6. I. Belykh, E. de Lange, M. Hasler, Physical review letters **94**(18), 188101 (2005)
7. M.E. Newman, Proceedings of the national academy of sciences **103**(23), 8577 (2006)
8. J. Stroud, M. Barahona, T. Pereira, in *Applications of Chaos and Nonlinear Dynamics in Science and Engineering-Vol. 4* (Springer, 2015)
9. D. Meunier, R. Lambiotte, E.T. Bullmore, Frontiers in neuroscience **4** (2010)
10. P.M. Gleiser, V.I. Spoomaker, Philosophical Transactions of the Royal Society of London A: Mathematical, Physical and Engineering Sciences **368**(1933), 5633 (2010)
11. C. Nicolini, A. Bifone, Scientific reports **6** (2016)
12. C. Assisi, M. Stopfer, M. Bazhenov, Neuron **69**(2), 373 (2011)
13. C.J. Honey, R. Kötter, M. Breakspear, O. Sporns, Proceedings of the National Academy of Sciences **104**(24), 10240 (2007)
14. D. Angulo-Garcia, J.D. Berke, A. Torcini, PLoS computational biology **12**(2) (2016)
15. A. Kumar, S. Rotter, A. Aertsen, Nature reviews. Neuroscience **11**(9), 615 (2010)
16. X. Yang, H. Li, Z. Sun, PloS one **12**(6), e0177918 (2017)
17. J. Hizanidis, N.E. Kouvaris, Z.L. Gorka, A. Díaz-Guilera, C.G. Antonopoulos, Scientific reports **6** (2016)
18. M. Santos, J. Szezech, F. Borges, K. Iarosz, I. Caldas, A. Batista, R. Viana, J. Kurths, Chaos, Solitons & Fractals **101**, 86 (2017)
19. J.L. Hindmarsh, R. Rose, Proceedings of the royal society of London B: biological sciences **221**(1222), 87 (1984)
20. R. Barrio, M. Angeles Martínez, S. Serrano, A. Shilnikov, Chaos: An Interdisciplinary Journal of Nonlinear Science **24**(2), 023128 (2014)
21. G. Innocenti, A. Morelli, R. Genesio, A. Torcini, Chaos: An Interdisciplinary Journal of Nonlinear Science **17**(4), 043128 (2007)
22. C. Van Vreeswijk, L. Abbott, G.B. Ermentrout, Journal of computational neuroscience **1**(4), 313 (1994)
23. T.J. Lewis, J. Rinzel, Journal of computational neuroscience **14**(3), 283 (2003)
24. C. Assisi, M. Bazhenov, Frontiers in neuroengineering **5** (2012)
25. C. Börgers, N. Kopell, Neural computation **15**(3), 509 (2003)
26. E. Catsigeras, International Journal of Bifurcation and Chaos **20**(02), 349 (2010)
27. G. Buzsáki, A. Draguhn, science **304**(5679), 1926 (2004)
28. X.J. Wang, G. Buzsáki, Journal of neuroscience **16**(20), 6402 (1996)
29. V.S. Sohal, J.R. Huguenard, Proceedings of the National Academy of Sciences of the United States of America **102**(51), 18638 (2005)
30. J.A. White, M.I. Banks, R.A. Pearce, N.J. Kopell, Proceedings of the National Academy of Sciences **97**(14), 8128 (2000)
31. R. Echeveste, C. Gros, Frontiers in computational neuroscience **10** (2016)
32. J. Rubin, M. Wechselberger, Chaos: An Interdisciplinary Journal of Nonlinear Science **18**(1), 015105 (2008)
33. T. Kispersky, J.A. White, H.G. Rotstein, PloS one **5**(11), e13697 (2010)
34. Y. Yamashita, J. Tani, PLoS computational biology **4**(11), (2008)
35. D. Papo, Frontiers in physiology **4** (2013)
36. K. Gupta, G. Ambika, The European Physical Journal B **89**(6), 147 (2016)
37. F. Siebenhühner, S.H. Wang, J.M. Palva, S. Palva, Elife **5**, e13451 (2016)
38. Y. Penn, M. Segal, E. Moses, Proceedings of the National Academy of Sciences **113**(12), 3341 (2016)
39. A. Borst, F.E. Theunissen, Nature neuroscience **2**(11), 947 (1999)
40. B.B. Averbeck, D. Lee, Trends in neurosciences **27**(4), 225 (2004)
41. R.B. Stein, Biophysical journal **7**(6), 797 (1967)
42. E.M. Izhikevich, N.S. Desai, E.C. Walcott, F.C. Hoppensteadt, Trends in neurosciences **26**(3), 161 (2003)
43. P. Tiesinga, T.J. Sejnowski, Neuron **63**(6), 727 (2009)
44. T. Womelsdorf, P. Fries, Current opinion in neurobiology **17**(2), 154 (2007)
45. R. Stoop, J. Buchli, M. Christen, in *Proceedings of the international symposium on nonlinear theory and its applications (NOLTA)* (2004)
46. E. Lowet, M. Roberts, A. Hadjipapas, A. Peter, J. van der Eerden, P. De Weerd, PLoS computational biology **11**(2), (2015)
47. C.C. Chow, J.A. White, J. Ritt, N. Kopell, Journal of computational neuroscience **5**(4), 407 (1998)